

Adsorption kinetics and isotherm of methylene blue and its removal from aqueous solution using bone charcoal

Gh. Ghanizadeh · G. Asgari

Received: 23 June 2010 / Accepted: 7 September 2010 / Published online: 1 October 2010
© Akadémiai Kiadó, Budapest, Hungary 2010

Abstract This study aims at describing the removal of methylene blue (MB) from aqueous solution using bone charcoal (BC) as an adsorbent material. The effects of dye concentration, pH, contact time and the adsorbent dose were investigated. The chemical composition and solid structure of BC were analyzed using X-ray diffraction (XRD) and scanning electronic microscopy (SEM). The surface area was measured via the Brunauer–Emmett–Teller (BET) isotherm. The experimental data were analyzed with Langmuir, Freundlich and Temkin isotherm models. The results show that the main component of BC is calcium hydroxylapatite ($\text{Ca}_5(\text{PO}_4)_3\text{OH}$). The BET_{Surface area} of BC is approximately 100 m²/g. The experimental adsorption isotherm complies with Langmuir equation model ($R^2 = 0.99$) and the maximum amount of adsorption (q_{max}) was 5 mg/g. The elevation of BC dose led to a decrease in q_{max} , however, increasing the pH led to the elevation of dye adsorption. The kinetic studies revealed that the adsorption of MB is rapid and complies with the pseudo second-order kinetic ($R^2 > 0.99$). Apart from R^2 , four error functions have been used for the validation of data. Analysis of data with Dubinin–Radushkevich isotherm showed that the energy of MB adsorption process onto BC was 2.65 kJ/mol, which implies that the adsorption of MB with BC is a physical adsorption.

Keywords Adsorption · Methylene blue · Dye removal · Bone charcoal

Gh. Ghanizadeh
Health Research Center and School of Health, Baqiyatallah University of Medical Sciences,
Tehran, I.R. Iran
e-mail: qanizadeh@yahoo.com

G. Asgari (✉)
Environmental Health Engineering Department, School of Public Health,
Hamadan University of Medical Sciences, Hamadan, I.R. Iran
e-mail: asgari@umsha.ac.ir

Introduction

Dyes are compounds that are widely used in textile, paper, plastic and cosmetic industries and are easily recognized as pollutants [1]. Methylene blue (MB) is a heterocyclic aromatic chemical compound. It has many uses in a range of different fields, such as biology and chemistry. At room temperature, it appears as a solid, odorless, dark green powder, which yields a blue solution when dissolved in water [2, 3].

Colored wastewater released into ecosystems is a dramatic source of esthetic pollution and perturbation in the aquatic ecosystems by its impending penetration of light as well as food web [1, 4]. Many dyes and their breakdown products may be toxic, carcinogenic and teratogenic for living organisms [5]. Thus, it is desirable to eliminate dyes from textile wastewater. The total dye consumption of textile industries alone is in excess of 10^7 kg/year and an estimated 90% of this total ends up on fabrics. Consequently, approximately 10^6 kg/year of various dyes is discharged into waste streams by the textile industries [6]. Due to the growing worldwide environmental regulations, the effluents of dye-contaminated industries have to be treated carefully before discharge [7]. Because of the complexity and the variety of dyes employed in dyeing processes, finding a unique treatment method that insures complete elimination of all types of dyes is difficult [8]. Although aerobic/anaerobic biological processes are the best alternative for the removal of a wide range of pollutants, some dyes and their degradation products may be toxic and, consequently, their treatment cannot depend on biodegradation alone. Thus, investigations have been conducted on the physicochemical processes for the removal of color from textile industrial wastewaters [9]. There are various methods for dye removal which include coagulation, chemical oxidation, photocatalytic degradation and membrane processes. However, all these methods have their own drawbacks and one or more limitations; and hence, none of them have been found successful in completely removing the color from wastewater [10].

Coagulation and flocculation using polyelectrolytes, lime, alum or ferrous salts produce metallic impurities and huge amounts of toxic sludge that pose handling and disposal problems, in addition to material costs [11]. Additionally, membrane processes that operate by transfer of the pollutants to another phase or by concentrating them rather than destroying them have similar limitations [8]. Amongst the numerous techniques of dye removal, the adsorption process is one of the effective processes that have been successfully employed for color removal from the wastewater [12]. Although activated carbon (AC) is a preferred sorbent for water and wastewater treatment, this material is expensive for many countries and its widespread use is restricted because of its high cost [2]. Additionally, AC has to be regenerated offsite with losses of about 10% in the thermal regeneration process. Various adsorbents like zeolites, polymeric resins, bentonite, peat and ion exchangers have been tested and used for the removal of dyes from textile industrial wastewaters [13]. This research focused on MB dye adsorption onto bone charcoal as a cheap adsorbent from aqueous solutions. The MB dye was chosen as an adsorbate/pollutant because it is known as an indicator of dye adsorption onto solid materials [2, 14]. A survey of studies shows that the removal of MB has been investigated with

several adsorbents; and since reports on adsorption/removal of MB dye with BC are not available, this research was carried out to investigate the adsorption kinetics and energy of adsorption process with BC for MB dye removal.

Experimental

Reagents and solutions

MB dye of analytical grade from Merck Company was used as an adsorbate; it was not purified prior to use. The molecular weight of MB is 373.9 g/mol, which corresponds to MB hydrochloride with three molecules of water ($C_{16}H_{18}N_3SCl \cdot 3H_2O$). MB dye was dried at 110 °C for 2 h before use [5]. Since the chemical characteristics of tap water and colored aqueous solutions are similar, the MB solution was prepared with tap water. All other chemicals were the guaranteed or analytic grade reagents commercially available and were used without further purification.

Preparation of bone charcoal (BC)

In this research, BC was prepared under laboratory conditions. The fresh bone from cattle and sheep was crushed into pieces of 10–15 cm in length, rinsed three times with water and boiled at least three times in water for 2 h to remove fat and residual protein pieces. The bone was dried at 100–110 °C overnight and cooled in a desiccator. The pyrolysis of crushed bones was carried out using a rectangular electrical furnace at 400 °C for 2 h. The solid brownish black yield was transported to the desiccator and cooled at room temperature. The pyrolyzed BC was pulverized by standard ASTM sieves with a 10–16 range mesh (1.18–2 mm) [15, 16].

Characterization of BC

The chemical composition and solid structure of BC was analyzed using X-ray diffraction (Philips) (XRD), scanning electronic microscopy (SEM) and energy dispersive analysis X-ray (EDAX) spectra (Model XL30 Philips). The results of these analyses are shown in Fig. 1. Other surface specifics of BC were characterized by several parameters like as pH_{ZPC} , $BET_{\text{surface area}}$, and iodine number which are presented in Table 1. The pH_{ZPC} of BC was determined using the pH drift method and batch equilibrium technique with 1:250 solid to liquid ratio in 0.01 M NaCl solution. Sodium chloride was used as an inert electrolyte. The initial pH of the NaCl solution was adjusted from 2 to 12 by adding NaOH and HCl (0.1 M) [17]. The suspensions were allowed to equilibrate for 48 h in an isothermal shaker (Model GFL 3017) with 120 rpm at 25 ± 1 °C. After suspensions were filtered using filter paper, the pH values were measured using a pH meter (Hach Co., USA). Also, in order to eliminate the influences of interferences a blank test was done [18]. The iodine number was determined by using a 0.05 M standardized iodine solution; titration was carried out using 0.1 M

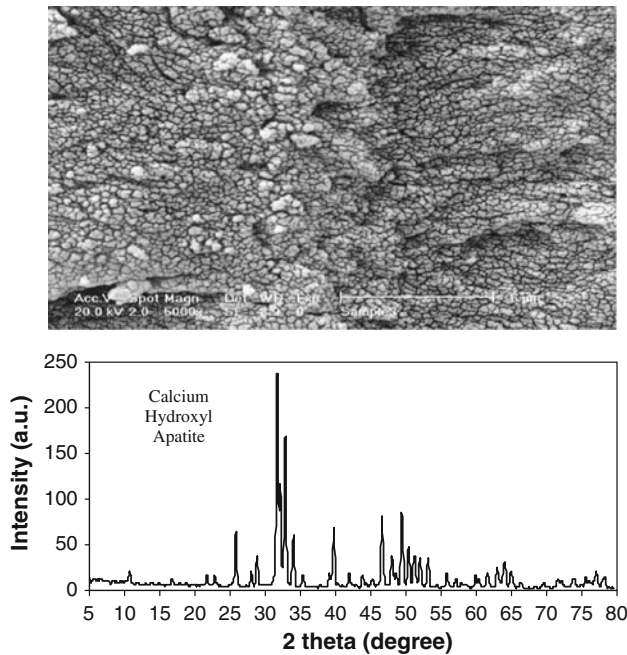


Fig. 1 SEM (20 kV, 5000 \times) and XRD of BC

Table 1 Bone charcoal characteristics

Specifications	Unit	Range
pH _{ZPC}	–	8.3
BET _{Surface area}	m ² /g	92.5
BJH _{Surface area}	m ² /g	116.41
Iodine number	mg/g	134.44
Pore volume	cm ³ /g	0.36
Pore size	nm	15.5
Size distribution	mm	1.18–2
D ₁₀	mm	1.08
D ₆₀	mm	1.72
Uniform coefficient (UC)	–	1.53

sodium thiosulfate [19]. The Brunauer–Emmett–Teller (BET) specific surface area and Barrett–Joyner–Halenda (BJH) specific surface area were determined by nitrogen adsorption–desorption measurement and by applying the linear BET-equation within P/P_0 0–1 [20]. Also, the porosity of BC was determined through the conventional adsorption of N₂ gas at 77 K and 91.43 kPa pressure [21]. Analysis of data for calculation of BET_{Surface area} and BJH_{Surface area} (m²/g), pore volume and porosity was carried out by Belsorb software (Ver.5) (data not shown).

Adsorption experiments

All the adsorption experiments were carried out by batch technique. Batch adsorption studies were performed at different doses of adsorbent, pH and dye concentrations. The initial concentration of the MB dye in the experiments was in the range of 50–200 mg/L. The dye solution (50 mL) of desired concentration at neutral pH was taken in amber and Al-covered glass vials and agitated with a known weight of BC at room temperature (25 ± 0.5 °C) in a shaker (GFL 3017) for a desired time period. Preliminary experiments demonstrated that the equilibrium established in about 120 min of contact time. Longer times gave practically the same uptake. Therefore, a contact time of 2 h was selected for the entire equilibrium test. The pH of the solution was carefully adjusted by adding a small amount of HCl and NaOH solutions (0.1 M) and measured using a pH meter. At the end of adsorption tests, the suspensions were centrifuged for 5 min at $2000 \times g$ and the concentrations of residual dye, C_e , were determined using a Philips UV/visible PU8700 spectrophotometer corresponding to λ_{\max} of MB that is 663 nm [5]. The concentration of dye in the solution was estimated quantitatively using of standard curve and its best line equation which was plotted on 663 nm. Blanks containing no dye were used for each series of experiments. Sampling was performed by removing 10 mL aliquots as grab samples and analyzed as above mentioned method. After adsorption of color onto BC, the prepared calibration curve can usually be used for dye measurement without dilution. The amount of adsorbed dye at equilibrium, q_e , and dye removal efficiency were calculated from the mass balance equation and Eq. 2:

$$q_e = \frac{V}{M} \times (C_0 - C_e) \quad (1)$$

$$E = \frac{C_0 - C}{C_0} \times 100 \quad (2)$$

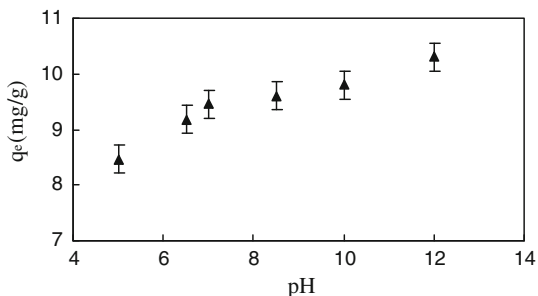
where C_e and C_0 are the equilibrium and initial concentrations of dye (mg/L); q_e is equilibrium dye concentration on adsorbent (mg/g), V is the volume of dye solution (L), M is the mass of BC sample used (g) and E is the removal efficiency [22–24]. The effect of adsorbent dosage was studied by varying the amount of BC from 0.3 to 10 g. All of the adsorption experiments were performed by agitation at 150 rpm at 25 ± 0.5 °C and the average of three replicates experiments was reported.

Result and discussion

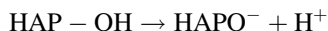
Effects of pH

Some properties of BC are presented in Table 1. As shown, based on the experimental results, the pH_{ZPC} of the BC was about 8.3. This adsorbent characteristic is very important, as it determines the point of pH at which the adsorbent surface has no net electrical charge. It has been reported that at any scale of pH below pH_{ZPC} , the surface

Fig. 2 Effect of pH on MB adsorption onto BC (conditions: BC dosage, 5 g/L; dye concentration, 300 mg/L; stirring speed, 150 rpm; $T = 25 \pm 0.5$ °C)



charge is positive; whereas, at pH level above pH_{ZPC} , the surface charge is negative [24]. Thus, this parameter has important effects on the adsorption process. Also, the pH of the aqueous solutions is a key factor in the adsorption process. Similar to pH_{ZPC} , this parameter plays an important role in chemical processes and affects the adsorption efficiency through the ionization of functional groups on the BC surface. The effects of solution pH on MB adsorption within BC were investigated and the results are illustrated in Fig. 2. It is observed that elevation of pH from 5 to 12 leads to an increase of MB adsorption capacity (q_e) from 8.5 to 10 mg/g. Based on this phenomenon, it can be derived that the elevation of aqueous pH to a higher scale than that of adsorbent pH_{ZPC} may lead to the increase of ionizable charge sites on the BC surface. At $pH > pH_{ZPC} = 8.3$, the HAP-surface hydroxyl groups of BC can be deprotonated in the following reaction:



Therefore, in the high pH range, the surface charge of BC is negative [25]. Al-Ghouti et al. [26] reported similar results and confirmed that an increase in aqueous pH leads to an increase in the maximum adsorption capacity of Jordanian diatomite and reported that an increase in pH from 4 to 11 leads to the decrease of surface charge from +0.136 to -0.022 C/m and an increase of MB dye adsorption [26]. Several studies show that MB has a positive charge in aqueous solutions [3, 27]; on the other hand, the increase of pH in aqueous solutions to higher than pH_{ZPC} leads to the increase of negative charge density on adsorbent surfaces, resulting in an increase of MB dye adsorption. As shown in Fig. 2, at any point of pH level above pH_{ZPC} , the adsorption of dye is higher than in other points. This phenomenon may be related to electrostatic interactions that appear between positive and negative charges of MB species and adsorbent surface, respectively. Also, it may be concluded that the increase of aqueous pH to higher than that of adsorbent pH_{ZPC} leads to the increase of current charges density within the adsorbate and adsorbent interface that can be related to the strength of Coulomb attractive forces and the higher adsorption of pollutants. Literature reports show several different views about the effect of pH on dye adsorption [27]. Bilgic [28] reported that a change in pH of MB solutions has no significant effect on the adsorption of MB within bentonite [29]. Ghosh and Bhattacharyya [29] reported that the MB adsorption on kaolinite has a minimum at around $pH = 4$.

Adsorbent characteristics

The results of XRD spectra (Fig. 1) demonstrated that the main component of BC is $\text{Ca}_5(\text{PO}_4)_3\text{OH}$. Also, an analysis of BC component with EDAX showed that calcium and phosphorous are predominant elements in BC structure (data not shown). These results show that the BC is a heterogeneous adsorbent which contains around 35% P and 57% Ca. Similar results were reported by Choy and Mc Kay [30]. The results of these researches show that the main structural component of BC is $\text{Ca}_5(\text{PO}_4)_3\text{OH}$. Also, Abe et al. [31] reported that BC structure contains 70–75% of calcium phosphate, which confirms the findings of the present investigation.

Although operational factors have a key role in adsorption processes, a survey of adsorption processes and adsorbent specificities shows that surface characteristics affect adsorption efficiency. Pyrolysis temperature and heating time hardly influence the surface characteristics of adsorbents. In this investigation, pyrolysis of BC was performed in 400 °C with 2 h residence time. Similar research confirmed that this condition is appropriate for BC pyrolysis. Mjengera and Mkongo [32] reported that BC prepared in 400 °C could be used to remove fluoride from water. This sorbent can also be used as a catalyst in ozonation systems for humic acid removal from water [33].

Analysis of surface characteristics with BJH model showed this adsorbent (BC) is not porous uniformly and the size of pores is less than 20 nm. Therefore, based on International Union of Pure and Applied Chemistry (IUPAC) classification, this adsorbent can be categorized as a microporous sorbent [21, 22].

Effect of dye concentration and contact time

From an economical point of view, the determination of the required contact time to reach equilibrium and the maximum concentration of pollutants that can be entered into adsorption systems are important in water and wastewater treatment. Fig. 3

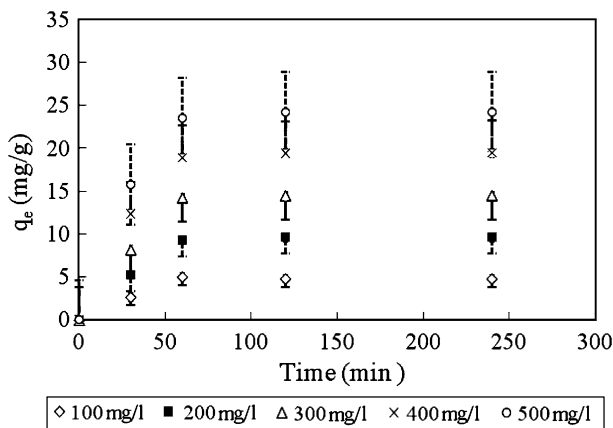


Fig. 3 Effect of dye concentration and contact time on MB adsorption (conditions: BC dosage, 5 g/L; stirring speed, 150 rpm; $T = 25 \pm 0.5$ °C; pH = 12)

shows the progress of MB dye adsorption versus the contact time and different concentrations of MB at room temperature. The quantity of adsorbed solute (mg/g) was increased with a lapse of contact time, and equilibrium was reached after 60 min. This figure shows the adsorption or migration rate of dye molecules from liquid to solid phase. As shown, the adsorption of pollutant has taken place in two stages where the first stage is faster than the second stage. This phenomenon can be confirmed with the slope of adsorption line that has the highest value in the first steps of reaction. Variation in the adsorption rate and the rise up to two different stages may be related to the presence of unoccupied surface areas that are most available in the first stages of dye adsorption.

As shown in Fig. 3, the increase of the preliminary concentration of MB leads to the elevation of the adsorbed mass of pollutant on BC. It is clear that the removal of MB with BC depends on the dye concentration. This phenomenon may be related to driving forces that need to be overcome for the resistances of mass transfer between the aqueous and solid phases. Similar results were reported for MB adsorption onto various adsorbents [34].

Effect of adsorbent dose

It is necessary that the effects of adsorbent dose are analyzed for the optimization and selection of the best required dose for scale-up and designing large scale equipments. In this research, variation of adsorbent dose showed that although an increase of BC dose in aqueous solution can result in the improvement of pollutant removal, this increase of BC leads to a decrease of adsorbed dye per unit of adsorbent (q_e). This phenomenon may be related to using surface area as unsaturated form. The results of this research showed that with increase of BC from 0.3 to 10 g, the q_e (mg/g) decreased from 32 to 1 mg/g (Fig. 4). This result implies that although the mass elevation of an adsorbent can provide a large available surface area, the adsorption pattern of the pollutant in its unsaturated form leads to an unfavorable use of the adsorbent [1, 10]. This phenomenon is most important in the design of economical and large scale adsorption devices. A comparison of the adsorption capacity of MB by the sorbent used in this work and those reported elsewhere is shown in Table 2. It is seen that the sorption capacity of the sorbent used in this work is still higher than some of the available ones in the literature.

Fig. 4 Variation of q_e versus adsorbent dosage (conditions: dye concentration, 300 mg/L; stirring speed, 150 rpm; $T = 25 \pm 0.5$ °C; pH = 12)

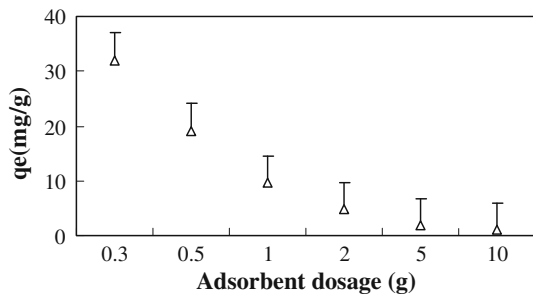


Table 2 Adsorption capacity of different sorbent for MB adsorption

Adsorbents	Capacity (mg/g)	Ref.
Jordanian diatomite	88–143	[26]
Activated tyres (850 °C)	1.3	[35]
Chrome sludge	0.51	[36]
Clay	6.3	[37]
Glass fiber	2.24	[38]
Fly ash	5.57	[39]
Silica	11.21	[37]
Bone charcoal	5	This study

Adsorption characteristics

In adsorption systems, the determination of the maximum adsorption capacity and development of an equation that could be accurately used for design purposes and optimization of economical equipments is important. Langmuir, Freundlich and Temkin models are among the most common isotherms that can be used for the description of solid–liquid sorption systems [11]. Linear regression analyses of these models and a comparison of their correlation coefficient (R^2) can be used for selection of the best fit isotherm. The Freundlich, Langmuir and Temkin isotherm equation can be represented respectively as below [11, 40]:

$$q_e = kc^n \quad (3)$$

A linear form of the Freundlich isotherm equation expression can be obtained by taking a logarithm:

$$\log q_e = \log k + \frac{1}{n} \log C_e \quad (4)$$

where q_e and C_e are parameters that are described in Eqs. 1 and 2. Constants k and n indicate the adsorption capacity and the adsorption intensity, respectively.

Also, the linear form of the Langmuir isotherm equation can be described as:

$$\frac{1}{q_e} = \frac{1}{q_{\max} \times bC_e} + \frac{1}{q_{\max}} \quad (5)$$

where q_{\max} is the maximum amount of adsorption (mg/g) and b is the adsorption equilibrium constant (L/mg).

The Temkin isotherm is represented by the following equation:

$$q_e = \frac{RT}{b} \text{Ln}(K_t C_e) \quad (6)$$

This equation can be expressed in linear form as:

$$q_e = B \text{Ln} K_t + B \text{Ln} C_e \quad (7)$$

where $B = (RT/b)$. T is the absolute temperature in K, and R is the universal gas constant in (J/molK). In this model, k_t is the binding constant which represents the maximum binding energy and constant B is related to the heat of adsorption [34].

The parameters of Freundlich and Langmuir models were determined with plots of $\log q_e$ versus $\log C_e$ and $(1/q_e)$ versus $(1/C_e)$. For the analysis of data with the Temkin model, the parameters of equation have been determined with plot of q_e versus $\ln C_e$.

Application of the Langmuir, Freundlich and Temkin models to the adsorption isotherm (Figs. 5, 6) showed that the Langmuir isotherm model turned out to be extremely satisfactory with the highest R^2 value (>0.99), compared to the other two

Fig. 5 Freundlich and Langmuir isotherm for the sorption of MB dye (conditions: stirring speed, 150 rpm; $T = 25 \pm 0.5$ °C; pH = 12)

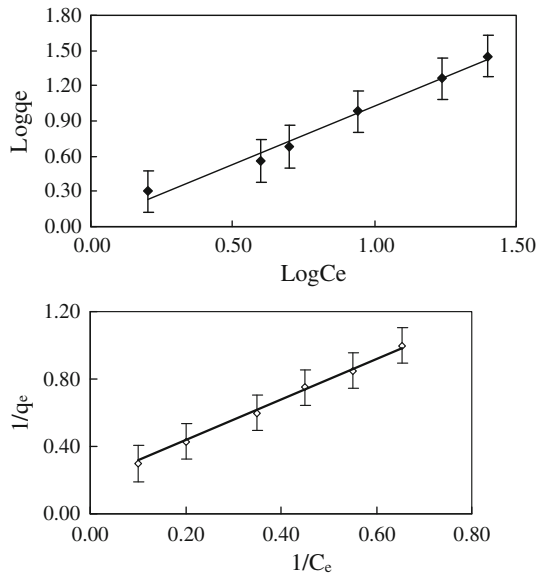


Fig. 6 Dubinin–Radushkevich and Temkin adsorption isotherm of MB onto BC (conditions: stirring speed, 150 rpm; $T = 25 \pm 0.5$ °C; pH = 12)

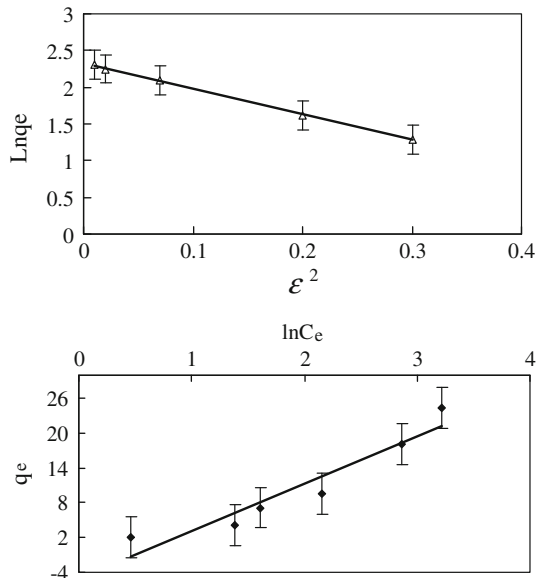


Table 3 The constants of isotherm models for MB adsorption within BC

	Freundlich	Langmuir	Temkin		
k (L/g)	1.26	b (L/mg)	0.167	k_t (L/mg)	1
n	0.92	q_{max} (mg/g)	5	B	8.11
R^2	0.98	R^2	0.99	R^2	0.90
MPSD	13.8	MPSD	8.69	MPSD	36.68
HYBRID	8.97	HYBRID	1.8	HYBRID	72

models. The estimated values for the parameters of these models were shown in Table 3.

The essential feature of the Langmuir isotherm can be described with dimensionless separation factor or equilibrium constant R_L that is used for the description of the adsorption condition which can be expressed as follows [41]:

$$R_L = \frac{1}{1 + bC_0} \tag{8}$$

where C_0 is the initial concentration of dye. The value of R_L represents the adsorption situations to be unfavorable ($R_L > 1$), linear ($R_L = 1$), favorable ($R_L < 1$) or irreversible ($R_L = 0$) [34, 42]. Based on the Langmuir constant, the value of this parameter for MB adsorption within BC is <1 which confirms that the adsorption of this dye with this material is favorable under the conditions of this study. It could be derived that the Langmuir isotherm gave better fits than the other isotherms, where the maximum uptake capacity for MB is 5 mg/g.

Validity of adsorption isotherm

Apart from correlation coefficient (R^2), Marquardt’s percent standard deviation (MPSD) and the hybrid error function (HYBRID) were also used to measure the goodness-of-fit. MPSD and HYBRID can be defined as:

$$MPSD = 100 \sqrt{\frac{1}{N - P} \sum_{i=1}^N \left(\frac{q_{ei}^{exp} - q_{ei}^{cal}}{q_{ei}^{exp}} \right)^2} \tag{9}$$

$$HYBRID = \frac{100}{N - P} \sum_{i=1}^N \left[\frac{(q_{ei}^{exp} - q_{ei}^{cal})^2}{q_{ei}^{exp}} \right] \tag{10}$$

where q_{ei}^{exp} is the observation from the batch experiment i , q_{ei}^{cal} is the estimated from the isotherm for corresponding q_{ei}^{exp} , N is the number of observations in experimental isotherm and P is the number of parameters in regression model. The smaller MPSD and HYBRID values reveal more accurate estimation of q_e value [43].

Kinetic parameters and energy of adsorption

The kinetic studies of adsorption processes provide useful information from the point of view of process efficiency and feasibility of scale-up operation parameters

for designing economical equipments. The kinetics of dye adsorption onto solid materials can be determined with different kinetic models. In this research, the kinetic of MB dye adsorption within BC was evaluated with the pseudo first-order and pseudo second-order models. For the analysis of data with the first model, the linear form of Lagergren equation was used which can be expressed as:

$$\frac{dq_t}{dt} = k_1(q_e - q_t) \quad (11)$$

The integrated form of this equation can be written as:

$$\log(q_e - q_t) = \log(q_e) - \frac{k_1}{2.203}t \quad (12)$$

where q_e and q_t are the amounts of dye adsorbed per unit weight of adsorbent (mg/g) at equilibrium time and time t , and k_1 is the rate constant for pseudo first-order kinetics. The value of this constant has been calculated from the plot of $\log(q_e - q_t)$ versus t . Several studies show that the first-order model may not fully describe the adsorption kinetics; so, in this study we used the pseudo second-order equations. This model is often successfully used to describe the kinetics of fixation reaction of adsorbate on adsorbent surface. The equation of this model can be described as:

$$\frac{dq_t}{dt} = k_2(q_e - q_t)^2 \quad (13)$$

The linear and integrated form can be expressed as:

$$\frac{t}{q_t} = \frac{1}{k_2q_e^2} + \frac{1}{q_e}t \quad (14)$$

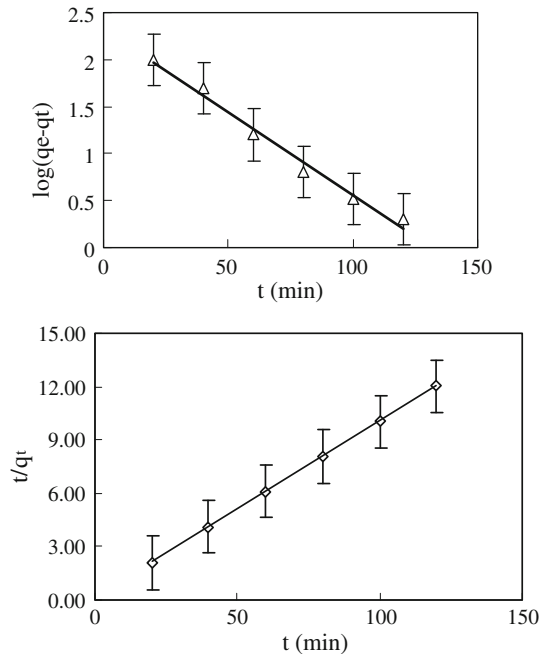
where k_2 is the rate constant of adsorption, q_e is the amount of MB adsorbed at equilibrium (mg/g) and q_t is the amount of adsorbed dye at time t (mg/g). The equilibrium adsorption capacity (q_e) and the rate constant k_2 (g/mg.min) can be determined with the plot of (t/q_t) versus t [44]. An analysis of data and regression coefficient (R^2) of Fig. 7 shows that the pseudo first-order kinetic model does not fit well with the MB adsorption onto BC ($R^2 = 0.98$) and the adsorption of this dye complies with the pseudo second-order kinetics. Because the correlation coefficient of this model is higher than 0.99, the calculated adsorption capacity complies with the experimental values. The values of k_1 and k_2 were calculated as 0.041 and 0.063 min^{-1} for pseudo first-order and pseudo second-order kinetics, respectively. Apart from the correlation coefficient (R^2), validation of kinetic models was been carried out by the normalized standard deviation (NSD), and average relative error (ARE) which are defined as:

$$\text{NSD} = 100 \sqrt{\frac{1}{N-1} \sum_{i=1}^N \left[\frac{(q_t^{\text{exp}} - q_t^{\text{cal}})}{q_t^{\text{exp}}} \right]^2} \quad (15)$$

$$\text{ARE} = \frac{100}{N} \sum_{i=1}^N \left| \frac{(q_e^{\text{exp}} - q_e^{\text{cal}})}{q_e^{\text{exp}}} \right|_i \quad (16)$$

where q_t^{exp} and q_t^{cal} (mg/g) are experimental and calculated MB adsorbed on BC at time t and N is the number of measurements made. The smaller NSD and ARE

Fig. 7 Pseudo first-order and pseudo second-order kinetics of MB adsorption onto BC



values indicate more accurate estimation of q_t values [43]. NSD and ARE values for pseudo first-order and pseudo second-order models are 3.74, 2.16 and 1.47, 0.57, which imply that the adsorption kinetics of MB onto BC can be described by the pseudo second-order model.

In adsorption studies, the determination of adsorption energy and understanding of adsorption type are most important. Since Langmuir and Freundlich isotherms do not give information about mechanisms and energy of adsorption, other isotherms should be used to determine the adsorption mechanism and energy of process. This information can be obtained using Dubinin–Radushkevich isotherm which can be expressed as:

$$\ln q_e = \ln q_{\max} - k\varepsilon^2 \quad (17)$$

where ε (Polanyi potential) is $RT \ln(1 + (1/C_e))$, q_{\max} the adsorption capacity (mg/g), k a constant related to adsorption energy, R and T are the gas constant and temperature (K) [41]. Fig. 6 shows the plot of $\ln q_e$ versus ε^2 . The value of ε can be calculated directly from related equation and k from the intercept of this curve. As mentioned above, k is related to energy adsorption, so the mean energy of adsorption (E) can be calculated from the k value using the following equation:

$$E = -(2k)^{-0.5} \quad (18)$$

Several studies show the mechanism of adsorption may be defined as physical or chemical that is related to energy of adsorption. The numerical value of energy is in the range of 1–8 and 9–16 kJ/mol for physical and chemical adsorption, respectively

[45]. In this research, the value of E was calculated to be 2.65 kJ/mol, which implies the adsorption of MB on BC is of physical type.

Conclusion

Surface characteristics and cheap availability of BC show that this material can be used as an adsorbent for the removal of environmental pollutants. The pH_{zpc} of this sorbent can provide good feasibilities for adsorption of cationic dye pollutants from alkaline aqueous solutions. Also, the potential of functional groups in the surface of BC for protonation and deprotonation is the most important characteristic that provides a good feasibility for the application of this adsorbent in the removal of cationic and anionic pollutants from aqueous solutions in the wide range of pH. A survey of adsorption isotherms of MB within BC showed that the adsorption of this dye complies with Langmuir isotherm in which the maximum adsorption capacity of BC is 5 mg/g and the kinetics of adsorption process was found to cope with the pseudo second-order model. Energy adsorption of MB shows that the adsorption of this dye onto BC is a physical sorption. Although the increase of BC dosage led to an increase in dye removal efficiency, the elevation of adsorbent mass on solution led to a decrease in q_{max} that is related to the unsaturation of adsorbent surface area with adsorbate. MB is known as a useful indicator of dye adsorption onto solid materials and BC has an appropriate capacity for its adsorption. Thus, this could be effectively applied as a low-cost adsorbent for the removal of dyes from wastewater in the adsorption processes.

Acknowledgment We are thankful to Prof. M. R. Naghii for his scientific comments and efforts in preparing of this article.

References

1. Ong ST, Lee CK, Zainal ZI (2007) Removal of basic and reactive dyes using ethylenediamine modified rice hull. *Bioresour Technol* 15:2792–2799
2. Attia AA, Girgis BS, Fathy NA (2008) Removal of methylene blue by carbons derived from peach stones by H_3PO_4 activation: batch and column studies. *Dyes Pigm* 76:282–289
3. Raposo F, De La Rubia MA, Borja R (2009) Methylene blue number as useful indicator to evaluate the adsorptive capacity of granular activated carbon in batch mode: influence of adsorbate/adsorbent mass ratio and particle size. *J Hazard Mater* 165:291–299
4. Daneshvar N, Khataee AR, Amani Ghadim AR, Rasoulifard MH (2007) Decolorization of C.I. Acid Yellow 23 solution by electrocoagulation process: investigation of operational parameters and evaluation of specific electrical energy consumption (SEEC). *J Hazard Mater* 148:566–572
5. Sariglu M, Aatay UA (2006) Removal of methylene blue by using biosolid. *J Glob Nest* 8:113–120
6. Hameed BH, Ahmed AA, Aziz N (2007) Isotherms, kinetics and thermodynamics of acid dye adsorption on activated palm ash. *Chem Eng J* 133:195–203
7. Lodha B, Chaudhari S (2007) Optimization of Fenton-biological treatment scheme for the treatment of aqueous dye solutions. *J Hazard Mater* 148:459–466
8. Mounir B, Pons MN, Zahraa O, Yaacoubi A, Benhammou A (2007) Discoloration of a red cationic dye by supported TiO_2 photocatalysis. *J Hazard Mater* 148:513–520
9. Al-Funaisi A, Jamrah A, Al-Hanai R (2007) Aspects of cationic dye molecule adsorption to Polygorskite. *Desalination* 214:327–342

10. Sulak MT, Demirbas E, Kobya M (2007) Removal of Astrazon Yellow 7GL from aqueous solutions by adsorption onto wheat bran. *Bioresour Technol* 13:2590–2598
11. Farah JY, EL-Gendy NS, Farahat LA (2007) Biosorption of Astrozone Blue Basic dye from an aqueous solution using dried biomass of Baker's yeast. *J Hazard Mater* 148:402–408
12. Dogen M, Abak H, Alkan M (2009) Adsorption of methylene blue onto hazelnut shell: kinetics and mechanism and adsorptive energy. *J Hazard Mater* 164:172–181
13. dos Santos AB, Cervantes FJ, van Lier JB (2007) Review paper on current technologies for decolourisation of textile wastewater: perspective for anaerobic technology. *Bioresour Technol* 98:2369–2385
14. Mehmet D, Mahir A, Aydın T, Yasemin O (2004) Kinetics and mechanism of removal of methylene blue by adsorption onto perlite. *J Hazard Mater B* 109:141–148
15. Purevsuren B, Avid B, Narangerel J, Gerellama T, Davaajav YA (2004) Investigation on the pyrolysis products from animal bone. *J Mater Sci* 39:737–740
16. Choy KKH, McKay G (2005) Sorption of metal ions from aqueous solution using bone charcoal. *Environ Int* 31:845–854
17. Orfão JJ, Silva AI, Pereira JC, Barata SA, Fonseca IM, Faria PC, Pereira MF (2006) Adsorption of a reactive dye on chemically modified activated carbons—influence of pH. *J Colloid Interface Sci* 296:480–489
18. Karthikeyan G, Ilango SS (2007) Fluoride sorption using Moringa Indica-based activated carbon. *Iran J Environ Health Sci Eng* 4:21–28
19. A.S.T.M. Book of Standards. D2862-97R04 (2007) Test method for particle size distribution of granular activated carbon, vol 15.01, 26th edn. ASTM International, West Conshohocken, pp 396–405
20. Vágvölgyi V, Kovács J, Horváth E, Kristóf J, Makó É (2008) Investigation of mechanochemically modified kaolinite surfaces by thermoanalytical and spectroscopic methods. *J Colloid Interface Sci* 317:523–529
21. Shieldes JE, Thomas MA, Thommes M (2004) Characterization of porous solids and powders: surface area, pore size and density. Kluwer Academic Publishers, The Netherlands, pp 58–63
22. MWH (2005) Water treatment: principles and design, 2nd edn. Wiley, New Jersey
23. Karaoğlu MH, Doğan M, Alkan M (2009) Removal of cationic dye by kaolinite. *Microporous Mesoporous Mater* 122:20–27
24. Rezaee A, Ghanizadeh G, Behzadiyannejad G, Yazdanbakhsh AR, Siyadat SD (2009) Adsorption of endotoxin from aqueous solution using bone charcoal. *Bull Environ Contam Toxicol* 6:732–737
25. Medellin-Castillo NA, Leyva-Ramos R, Ocampo-Perez R, de la Garcia RF, Aragon-Pina A, Martínez-Rosales JM (2007) Adsorption of fluoride from water solution on bone char. *Ind Eng Chem Res* 46:9205–9212
26. Al-Ghouti MA, Khraisheh MAM, Ahmad MNM, Allen S (2009) Adsorption behaviour of methylene blue onto Jordanian diatomite: a kinetic study. *J Hazard Mater* 165:589–598
27. Doğan M, Karaoğlu MH, Alkan M (2009) Adsorption kinetics of maxilon yellow 4GL and maxilon red GRL dyes on kaolinite. *J Hazard Mater* 165:1142–1151
28. Bilgiç C (2005) Investigation of the factors affecting organic cation adsorption on some silicate minerals. *J Colloid Interface Sci* 281:33–38
29. Ghosh D, Bhattacharyya KG (2002) Adsorption of methylene blue on kaolinite. *Appl Clay Sci* 20:295–300
30. Choy KKH, McKay G (2005) Sorption of cadmium, copper, and zinc ions onto bone char using Crank diffusion model. *Chemosphere* 60:1141–1150
31. Abe I, Iwasaki S, Tokimoto T, Kawasaki N, Nakamura T, Tanada S (2004) Adsorption of fluoride ions onto carbonaceous materials. *J Colloid Interface Sci* 275:35–39
32. Mjengera H, Mkongo G (2003) Appropriate deflouridation technology for use in flourotic areas in Tanzania. *Phys Chem Earth Parts A/B/C* 28:1097–1104
33. Mortazavi SB, Asgari Gh, Hashemian SJ, Moussavi G (2010) Degradation of humic acids through heterogeneous catalytic ozonation with bone charcoal. *Reac Kinet Mech Cat* 100:471
34. Hameed BH, Ahmad AA (2009) Batch adsorption of methylene blue from aqueous solution by garlic peel, an agricultural waste biomass. *J Hazard Mater* 164:870–875
35. Woolard CD, Strong J, Erasmus CR (2002) Evaluation of the use of modified coal ash as a potential sorbent for organic waste streams. *Appl Geochem* 17:1159–1164
36. Banat F, Al-Asheh S, Al-Ahmad R, Bni-Khalid F (2007) Bench-scale and packed bed sorption of methylene blue using treated olive pomace and charcoal. *Bioresour Technol* 98:3017–3025

37. Tamez Uddin Md, Akhtarul Islam Md, Mahmud S, Rukanuzzaman Md (2009) Adsorptive removal of methylene blue by tea waste. *J Hazard Mater* 164:53–60
38. Chakrabarti S, Dutta BK (2005) On the adsorption and diffusion of methylene blue in glass fibers. *J Colloid Interface Sci* 286:807–811
39. Vasanth Kumar K, Ramamurthi V, Sivanesan S (2005) Modeling the mechanism involved during the sorption of methylene blue onto fly ash. *J Colloid Interface Sci* 284:14–21
40. AWWWW (1999) Water quality and treatment. In: Pontius FW (ed) A handbook of community water supplies, 4th ed. Mac Graw-Hill, Inc., Washington, DC, pp 613–781
41. Bayramoglu G, Altintas B, Arica MY (2009) Adsorption kinetics and thermodynamic parameters of cationic dyes from aqueous solutions by using a new strong cation-exchange resin. *Chem Eng J* 152:339–346
42. Ghanizadeh Gh, Ehrampoush MH, Ghaneian MT (2010) Application of iron impregnated activated carbon for removal of arsenic from water. *Iran J Environ Health Sci Eng* 7:145–156
43. Behnamfard A, Salarirad MM (2009) Equilibrium and kinetic studies on free cyanide adsorption from aqueous solution by activated carbon. *J Hazard Mater* 170:127–133
44. Yu J, Li X, Sun B, Jun Y, Chi R (2009) Adsorption of methylene blue and rhodamine B on baker's yeast and photocatalytic regeneration of the biosorbent. *Biochem Eng J* 45:145–151
45. Kundu S, Gupta AK (2007) Adsorption characteristics of As(III) from aqueous solution on iron oxide coated cement (IOCC). *J Hazard Mater* 142:97–104